arXiv:hep-ph/0605233v4 21 Sep 2006

IMSc-2006/05/22

$\overline{B}_s \to \mu^+\mu^-$ decay in the Randall-Sundrum model

Basudha Misra [1], Jyoti Prasad Saha [2]
and
Prasanta Kumar Das [3]

The Institute of Mathematical Sciences,
C.I.T Campus, Taramani,
Chennai 600113, India.

Abstract

We investigate the $\overline{B}_s \to \mu^+\mu^-$ decay in the presence of a light stabilized radion in Randall-Sundrum model. The branching ratio $BR(\overline{B}_s \to \mu^+\mu^-)$ in the standard model is found to be 3.17×10^{-9} (two order smaller than the experimental upper bound) and raises the question whether some new physics can play a crucial role or not. We found that for a reasonable range of parameters (i.e. radion mass m_ϕ and radion vev $\langle\phi\rangle$), the above deficit between the experimental bound and the standard model result can well be accomodated. Using this upper bound on $BR(\overline{B}_s \to \mu^+\mu^-)$, we obtain the lower bound on $\langle\phi\rangle$.

Keywords: $\overline{B}_s$-meson, Rare decay, Extra dimensional field theory.

PACS Nos.: 14.40.Nd;12.60.-i;11.10.Kk.

---

[1] E-mail: basudha@imsc.res.in

[2] E-mail: jyoti@imsc.res.in

[3] E-mail: dasp@imsc.res.in

1 Introduction

The standard model(SM) despite it's enormous experimental success, succumbs some serious drawbacks as far as our understandings of the flavour structure of the quarks and leptons are concerned. The CKM matrix, telling a lot about the mixing and CP-violation in the quark sector, lacks any dynamical mechanism in it's origin. Simlilarly, the neutrino masses and mixing which is absent in the SM, requires the existence of beyond SM physics. An urge for going beyond the SM (by invoking new physics(NP)) has become a driving force behind most of the present phenomenological studies. Ideas like supersymmetry (with or without R-parity), technicolor, extra-dimensional field theory, split fermion as a candidate of NP draw a lot of attention among the physics community and the result is that the LANL archive is flourished by thousands of paper in each year. Among several ingenious ideas the notion of extra spatial dimension(s) ([1], [2]) have become very popular as they partially resolve hierarchy puzzle. Among these the Randall-Sundrum(RS) model (of warped extra spatial dimension) is particularly interesting from the phenomenological point of view. This model views the world as 5-dimensional and it's fifth spatial dimension is S^1/Z_2 orbifold. The metric describing such a world can be written as

$$ds^2 = \Omega^2 \eta_{\mu\nu} dx^\mu dx^\nu - R_c^2 d\theta^2. \tag{1}$$

The pre-factor $\Omega^2 = e^{-2kR_c|\theta|}$ appearing in above is called the warp factor. In Ω^2, k stands for the bulk curvature constant and R_c for the size of the extra dimension. The angular variable θ parametrizes the fifth dimension ($x_5 = R_c\theta$). The model is constructed out of two D_3 branes located at the two orbifold fixed points $\theta = 0$ and $\theta = \pi$, respectively. The brane located at $\theta = 0$ (where gravity peaks) is known as the Planck brane, whereas the brane located at $\theta = \pi$ (on which the SM fields resides and the gravity becomes weak) is called the TeV brane.

The radius R_c can be related to the vacuum expectation value (vev) of some modulus field $T(x)$ which corresponds to the fluctuations of the metric over the background geometry (given by R_c). Replacing R_c by $T(x)$ we can rewrite the RS metric at the orbifold point $\theta = \pi$ as

$$ds^2 = g^{vis}_{\mu\nu} dx^\mu dx^\nu, \tag{2}$$

where $g^{vis}_{\mu\nu} = e^{-2\pi kT(x)}\eta_{\mu\nu} = \left(\frac{\phi(x)}{f}\right)^2 \eta_{\mu\nu}$. Here $f^2 = \frac{24M_5^3}{K}$, where M_5 is the 5-dimensional Planck scale [2] and $\phi(x) = fe^{-\pi kT(x)}$. The scalar field $\hat{\phi}(x)$ (i.e. $\hat{\phi}(x) = \phi(x) - \langle\phi\rangle$) is known as the radion field. In the minimal version of the RS model there is no potential which can stabilize the modulus field $T(x)$ (and thus the radion $\hat{\phi}(x)$). However in a pioneering work, Goldberger and Wise [3] were able to generate a potential of this modulus field (by adding an extra massive bulk scalar) field which has the correct minima satisfying $kR_c \simeq 11 - 12$, a necessary condition for the hierarchy resolution.

In this non-minimal RS model (RS model together with the Goldberger and Wise mechanism), the stabilzed radion can be lighter than the other low-lying gravitonic degrees of freedom and will reveal itself first either in the direct collider search or indirectly through the precission measurement. Studies based on the observable consequences of radion are available in the literature ([4]).

However, the impact of radion in heavy B meson decay, particularly in the rare decay mode, is not fully explored and the present work is an effort in that direction. We have investigated the rare $\overline{B}_s \to \mu^+\mu^-$ mode in the light of a stabilized radion. The branching ratio $BR(\overline{B}_s \to \mu^+\mu^-)$

within the SM is found to be two order smaller than the experimental upper bound 1.0×10^{-7} [5]. It is worthwhile to see whether this deficit can be accommodated within this brane world model.

The organization of the paper is as follows. In Section 2 we obtain the $BR(\overline{B}_s \to \mu^+\mu^-)$ within the standard model and in the presence of a light stabilized radion. We discuss several input parameters: CKM matrix elements, quark and lepton masses, effective wilson coefficients, decay constants in Section 3. Section 4 is fully devoted to the numerical analysis. Here we show how the upper bound of $BR(\overline{B}_s \to \mu^+\mu^-)$ can give some lower bound on radion vev $\langle\phi\rangle$ for a relatively light radion. We summarize and conclude in Section 5.

2 The exclusive rare $\overline{B}_s \to \mu^+\mu^-$ decay

2.1 Standard Model(SM)

The $\overline{B}_s(p_B) \to \mu^+(p_1)\mu^-(p_2)$ (partonically described as the $b\overline{s} \to \mu^+\mu^-$ FCNC transition) decay within the SM is found to be two order smaller than the experimental upper bound. This channel can be useful to test certain class of New Physics, particularly the notion of warped geometry by probing it's moduli (radion).

To begin with let us recall the result of the $\overline{B}_s \to \mu^+\mu^-$ decay in the standard model [6]. The QCD improved effective Hamiltonian $\mathcal{H}_{\rm eff}$ describing such a $\Delta B = 1$ transition can be written as

$$\mathcal{H}_{\rm eff} = \frac{G_F}{\sqrt{2}}\left[V_{tb}V_{ts}^*\left(c_7^{eff}O_7 + c_9^{eff}O_9 + c_{10}O_{10}\right)\right], \tag{3}$$

where the operators $O_i(\ i = 9, 10)$ (semileptonic operators involving electro-weak (γ, Z) penguin and box diagram) and O_7 (magnetic penguin) [6, 7] are given by,

$$\begin{aligned} O_9 &= \frac{\alpha}{\pi}(\overline{s}\gamma_\mu P_L b)(\overline{\mu}^-\gamma^\mu\mu^+), \\ O_{10} &= \frac{\alpha}{\pi}(\overline{s}\gamma_\mu P_L b)(\overline{\mu}^-\gamma^\mu\gamma_5\mu^+), \\ O_7 &= \frac{\alpha}{\pi}(\overline{s}\sigma_{\mu\nu}q^\nu P_R b)\left[\frac{-2im_b}{q^2}\right](\overline{\mu}^-\gamma^\mu\mu^+). \end{aligned} \tag{4}$$

Here $\sigma_{\mu\nu} = \frac{i}{2}[\gamma_\mu, \gamma_\nu]$, the chiral-projection operators $P_{R,L} = \frac{1}{2}(1 \pm \gamma_5)$. $\alpha = \frac{e^2}{4\pi}$ is the QED fine structure constant. In above q is the momentum transferred to the lepton pair, m_b, the b-quark mass. Since we are considering the $\overline{B}_s$ meson, the matrix element of $\mathcal{H}_{\rm eff}$ is to be taken between the vacuum and $|\overline{B}_s\rangle$ state. Defining $f_{\overline{B}_s}$ as the decay constant of the $\overline{B}_s$ meson, we find [7]

$$\langle 0|\overline{s}\gamma^\mu\gamma^5 b|\overline{B}_s(p_B)\rangle = if_{\overline{B}_s}p_B^\mu, \tag{5}$$

$$\langle 0|\overline{s}\gamma^5 b|\overline{B}_s(p_B)\rangle = \frac{-if_{\overline{B}_s}m_{\overline{B}_s}^2}{m_b + m_s}, \tag{6}$$

and

$$\langle 0|\overline{s}\sigma^{\mu\nu}P_R b|\overline{B}_s(p_B)\rangle = 0. \tag{7}$$

Since $q = p_1 + p_2$, the c_9^{eff} term in Eqn.(3) gives zero contribution on contraction with the lepton bilinear, c_7^{eff} gives zero by Eqn.(7) and the remaining c_{10} gives a contribution given by

$$\begin{aligned} iM_{SM}(\overline{B}_s(p_B) \to \mu^+(p_1)\mu^-(p_2)) &= iM_{10}(\overline{B}_s(p_B) \to \mu^+(p_1)\mu^-(p_2)) \\ &= i\frac{G_F}{\sqrt{2}} V_{tb}V_{ts}^* c_{10} \langle \mu^+(p_1)\mu^-(p_2)|O_{10}|\overline{B}_s(p_B)\rangle, \end{aligned} \tag{8}$$

where O_{10} is given in Eq. (4). Accordingly the decay amplitude square is given by

$$\overline{|M_{SM}|^2} = \overline{|M_{10}|^2}. \tag{9}$$

For the explicit expression of $\overline{|M_{10}|^2}$ see Appendix A.

2.2 New Physics(NP) (moduli/radion contribution)

The light stabilized radion $\hat{\phi}(x)$ can potentially be significant in the $\overline{B}_s \to \mu^+\mu^-$ decay. Since gravitational interaction conserves flavour, radion can not cause flavour-changing neutral current (FCNC) transition $b \to s$ at the tree level and it can happen only at the loop level which we will see shortly. The radion interaction with the SM fields (which lives on the TeV brane) is governed by the 4 dimensional general coordinate invariance. It couples to the trace of the energy-momentum tensor $T^\mu_\mu(SM)$ of the SM fields and is given by

$$\mathcal{L}_{int} = \frac{\hat{\phi}}{\langle\phi\rangle} T^\mu_\mu(SM). \tag{10}$$

Here $\langle\phi\rangle$ is the radion vev and $T^\mu_\mu(SM)$ is

$$\begin{aligned} T^\mu_\mu(SM) = \sum_\psi \left[\frac{3i}{2}\left(\overline{\psi}\gamma_\mu D_\nu\psi - D_\nu\overline{\psi}\gamma_\mu\psi\right)\eta^{\mu\nu} - 4m_\psi\overline{\psi}\psi\right] - 2M_W^2 W_\mu^+ W^{-\mu} - m_Z^2 Z_\mu Z^\mu \\ +(2m_h^2 h^2 - \partial_\mu h \partial^\mu h) + ... \end{aligned} \tag{11}$$

where $D_\mu\psi = (\partial_\mu - ig\frac{\tau^a}{2}A^a_\mu - ig'\frac{Y_W}{2}B_\mu)\psi$ (τ^a's being the Pauli matrices, g, g' being $SU(2)_L$ and $U(1)_Y$ gauge coupling constants and Y_W, the weak hypercharge). Clearly Eq.(11) manifests that radion intercation with matter conserves flavour at the tree level. The Feynman rules comprising radion interactions with the SM fields are listed in Appendix B.1 (see Figure 1). For vertices involving radion-goldstone-goldstone, radion-goldstone-W boson, radion-fermion-antifermion-goldstone, radion-fermion-antifermion-W boson, we read the Feynman rule for vertices [8] without the radion and then just multiply the factor $1/\langle\phi\rangle$ to get the desired Feynman rule. For other vertices, the Feynman rules are directly read from Eq. (10). Now a b quark can decay to a s quark together with a ultra-light radion(ϕ, dropping the hat from $\hat{\phi}(x)$ from now and onwards) followed by the $\phi \to l^+l^-$ ($l = e, \mu$) decay. Since radion coupling to a pair of fermion (on-shell) is proportional to the fermion mass and $m_e = m_\mu \times 10^{-3}$, we do not consider the $\phi \to e^+e^-$ decay channel (and thus $\overline{B}_s \to e^+e^-$ decay mode) in our analysis, as it will not lead to useful bound on $\langle\phi\rangle$. At this point we should note that a virtual radion of heavier mass (say about few hundred GeV), might appears to be an interesting option. However, the possibility of FCNC transition (like $b \to s$ transition) with the radion, the real gravi-scalar, is ruled out. Note that an ultra-light radion of mass about $1 \sim 4$

GeV is not ruled out as far as the neutrino oscillaton inside supernova is concerned (see Ref.[9]). In Ref. [9], the authors showed that the radion exchange (potential) between the neutrino and the supernova matter will not effect the neutrino oscillation inside the supernova, yielding a lower bound on m_ϕ about 1 GeV. Another thing which requires attention is the possibility of having the radion $\phi(x)$ mixing with the higgs $h(x)$ field. A term like

$$S = -\zeta \int d^4x \sqrt{-g_{vis}}\; g^{\mu\nu}_{vis}\; H^\dagger H,$$

with $H^\dagger = \begin{pmatrix} 0 & (v + h(x))/\sqrt{2} \end{pmatrix}$ (with $v = 247$ GeV, the EW vev), can cause radion-higgs mixing [10]. However, here we confine ourselves in no-mixing scenario (i.e. we set ζ, the radion-higgs mixing parameter equal to zero). Analysis in a general radion-higgs mixing scenario is underway. The Feynman diagrams contributing to the $b \to s\phi$ FCNC transition are shown in Figure 2 (see Appendix B.2).

It is now straightforward to evaluate those diagrams and the effective operator parametrizing the radion contribution to $b \to s\phi$ process can be written as

$$O_{12} = V_{CKM}\, \frac{G_F}{\sqrt{2}}\, \mathcal{L}_\phi\, [m_b \bar{s} P_R b + m_s \bar{s} P_L b], \tag{12}$$

where $V_{CKM} = V^*_{is} V_{ib} (i = u, c, t)$, $G_F (= \frac{g^2\sqrt{2}}{8M_W^2})$, the Fermic constant. $\mathcal{L}_\phi$, the effective loop integral factor takes the form

$$\mathcal{L}_\phi = \frac{m_i^2}{2\pi^2 \langle\phi\rangle} \int_0^1 dx \left[4\; Log\left(\frac{\Lambda^2}{A^2}\right) - 4 + x\frac{m_i^2}{A^2} + \frac{(1-x)M_W^2}{A^2} \right], \tag{13}$$

in the t'Hooft-Feynman gauge $\xi = 1$ and $A^2 = x m_i^2 + (1-x) M_W^2$. In Eq. (13) i runs over u, c and t quarks, but in our analysis we set $i = t$ (since $m_t \gg m_u, m_d$). In evaluating $\mathcal{L}_\phi$ we assume that there is no external momentum flow (actually the external momenta is much smaller than the internal masses M_W and m_t and hence setting the external momentum to zero is a good approximation). Note that, the Figures 2(b,e,i,j) contribute in $b \to s\phi$ vertex (Eq. (13)), while the rest are not. We use the cut-off regularizing technique in regularizing the loop integral with the UV cut-off being $\Lambda = 4\pi\langle\phi\rangle$ (follows from naive-dimensional analysis).

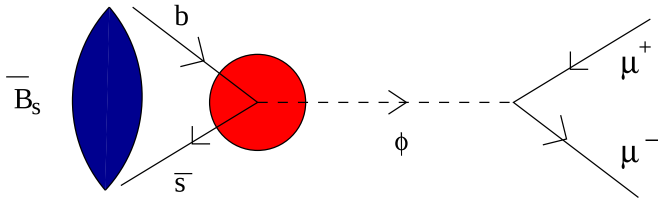

Figure 3. *Radion contribution to $\overline{B}_s(p_B) \to \mu^+(p_1)\mu^-(p_2)$decay. Momentum conservation (for the semileptonic process $b(p_b)\bar{s}(p_s) \to \mu^+(p_1)\mu^-(p_2)$) reads $p_B = p_b + p_s = p_1 + p_2$. The red blob corresponds to the effective $b - \bar{s} - \phi$ vertex.*

In finding the NP (radion) contribution to $\overline{B}_s \to \mu^+\mu^-$ decay, we neglect the m_s dependent term in Eq.(12) (since $m_s \ll m_b$). It is now straightforward to include the NP contribution to the $\overline{B}_s \to \mu^+\mu^-$ decay amplitude. The relevant new physics Feynman digram is shown in Figure 3 and the squared-amplitude $\overline{|M_{SM} + M_{NP}|^2}(\overline{B}_s \to \mu^+\mu^-)$ is given by

$$\overline{|M_{SM} + M_{NP}|^2} = \overline{|M_{10}|^2} + \overline{|M_{NP}|^2} + \overline{2Re(M_{10}^{\dagger} M_{NP})}. \tag{14}$$

The direct and interference terms of the amplitude (Eq.(14)) is presented in the Appendix A and B.3. Note that, in Figure 3 the radion ϕ, produced in the annihilation of b and $\overline{s}$ quarks, decays into $\mu^+\mu^-$ pairs. We are working in the Breit-Wigner approximation and in this approximation the radion propagator takes the form

$$\Delta_\phi = \frac{1}{\Big[(q^2 - m_\phi^2) + i m_\phi \Gamma_\phi\Big]}. \tag{15}$$

Here $q^2 = (p_b + p_s)^2 = (p_1 + p_2)^2$ and Γ_ϕ is the total width of the radion arising from it's decay $\phi \to f\overline{f}(f = u, d, c, s, t, b, e, \mu, \tau, \nu_e, \nu_\mu, \nu_\tau)$, WW, ZZ, hh (for the radion decay width and it's branching ratio to several channels see Ref. [11]).

Considering the NP contribution, the total decay width $\Gamma(\overline{B}_s \to \mu^+\mu^-)$ can be written as

$$\Gamma(\overline{B}_s \to \mu^+\mu^-) = \frac{p_c}{8\pi m_{\overline{B}_s}^2} \overline{|M_{TOT}|^2}, \tag{16}$$

where $\overline{|M_{TOT}|^2} = \overline{|M_{SM} + M_{NP}|^2}$ (as given above (Eq. 14)). p_c is the center of mass (c.o.m) momenta of the two charged muons in the $\overline{B}_s$ rest frame and is given by

$$p_c = \frac{\sqrt{\Big(m_{\overline{B}_s}^2 - (m_{\mu^+} - m_{\mu^-})^2\Big)\ \Big(m_{\overline{B}_s}^2 - (m_{\mu^+} + m_{\mu^-})^2\Big)}}{2 m_{\overline{B}_s}}. \tag{17}$$

Finally the branching ratio $BR(\overline{B}_s \to \mu^+\mu^-)$ is given by

$$BR(\overline{B}_s \to \mu^+\mu^-) = \tau_{\overline{B}_s} \Gamma(\overline{B}_s \to \mu^+\mu^-), \tag{18}$$

where $\tau_{\overline{B}_s} (= 1.461 \times 10^{-12}\ sec)$ is the life-time of the $\overline{B}_s$ meson [12].

3 Input parameters

The decay amplitudes depend on the CKM matrix elements, wilson coefficients, quark and lepton masses and the non-perturbative input like decay constants.

3.1 CKM matrix elements, quark masses, wilson coefficients and decay constant

We adopt the Wolfenstein parametrization with parameters A, λ, ρ and η of the CKM matrix as below

$$V_{CKM} = \begin{pmatrix} V_{ud} & V_{us} & V_{ub} \\ V_{cd} & V_{cs} & V_{cb} \\ V_{td} & V_{ts} & V_{tb} \end{pmatrix} = \begin{pmatrix} 1 - \frac{1}{2}\lambda^2 & \lambda & A\lambda^3(\rho - i\eta) \\ -\lambda & 1 - \frac{1}{2}\lambda^2 & A\lambda^2 \\ A\lambda^3(1 - \rho - i\eta) & -A\lambda^2 & 1 \end{pmatrix}. \tag{19}$$

We set A and $\lambda = \sin\theta_c$ (θ_c, the Cabibbo mixing angle) at 0.801 and 0.2265 respectively, in our analysis. Other relevant parameters are $\rho = \sqrt{\overline{\rho}^2 + \overline{\eta}^2}\ cos\gamma$ and $\eta = \sqrt{\overline{\rho}^2 + \overline{\eta}^2}\ sin\gamma$, where $\sqrt{\overline{\rho}^2 + \overline{\eta}^2} = 0.4048$ and $\gamma \simeq 62^o$ [13]. The quark masses(in GeV unit) are being set at their current values i.e. $m_u = 0.2,\ m_d = 0.2,\ m_s = 0.2,\ m_c = 1.4,\ m_b = 4.8,\ m_t = 175$ GeV [7] and $m_\mu = 0.105$ GeV. For the $\overline{B}_s$ meson we use $m_{\overline{B}_s} = 5.369$ GeV [12] and the decay constant $f_{\overline{B}_s} = 0.20$ GeV [14]. For our numerical calculation we use $c_{10} = -4.5461$ [7].

4 Numerical Analysis: Results and Discussions

The branching ratio $BR(\overline{B}_s \to \mu^+\mu^-)_{SM}$ in the Standard Model is found to be two order smaller [6] than the present experimental upper bound 1.0×10^{-7} [5]. Assuming that the future data (not the upper bound) will still differ from the SM result, it is thus worthwhile to see whether radion can explain the discrepency. Our analysis is organized as follows:

We first obtain the SM result. Using several numerical inputs (discussed in section 3), we find

$$BR(\overline{B}_s \to \mu^+\mu^-)_{SM} = 3.17 \times 10^{-9}, \tag{20}$$

which is two order smaller than the present experimental upper bound. Next we will see whether the radion can explain the above deficit or not.Taking into account the radion contribution along with the SM contribution, we find the total branching ratio which is given by Eq. (18) and is solely a function of the new physics parameters: (1) radion mass m_ϕ and (2) radion vev $\langle\phi\rangle$. In our analysis, we treat the radion as an ultra-light object whose mass m_ϕ varies in between $2m_\mu$ GeV to m_{B_s} GeV and in this mass range it's decay width is found to be quite small. We set it at $\Gamma_\phi = 0.001$ GeV (see [11] for an elaborate discussion on radion decay width).

Now let us define a quantity $R = \frac{BR(\overline{B}_s \to \mu^+\mu^-)}{BR(\overline{B}_s \to \mu^+\mu^-)_{SM}}$ which is a function of m_ϕ and $\langle\phi\rangle$, the two NP parameters(as mentioned above). R, which is purely to be determined from the experiment, can be potentially quite significant in radion discovery.

Since at present no data for $BR(\overline{B}_s \to \mu^+\mu^-)$ is available (only upper bound exists), we take the conservative viewpoint and we use R to impose constraints on m_ϕ and $\langle\phi\rangle$. What we do is as follows:

- We set $R = 10,\ 50$ and 100 and use those to obtain contour plots in the $m_\phi - \langle\phi\rangle$ plane, which are shown in Figure 4a. The topmost, middle and lowermost curves respectively stands for $R = 10, 50$ and 100. In Figure 4b we have plotted R as a function of m_ϕ and $\langle\phi\rangle$.
- From Figure 4a we can see that the lower bound on $\langle\phi\rangle$ for a given m_ϕ decreases with the increase in R. For $R = 10(50, 100)$ and $m_\phi = 2$ GeV, we find $\langle\phi\rangle \geq 918(564, 459)$ GeV.

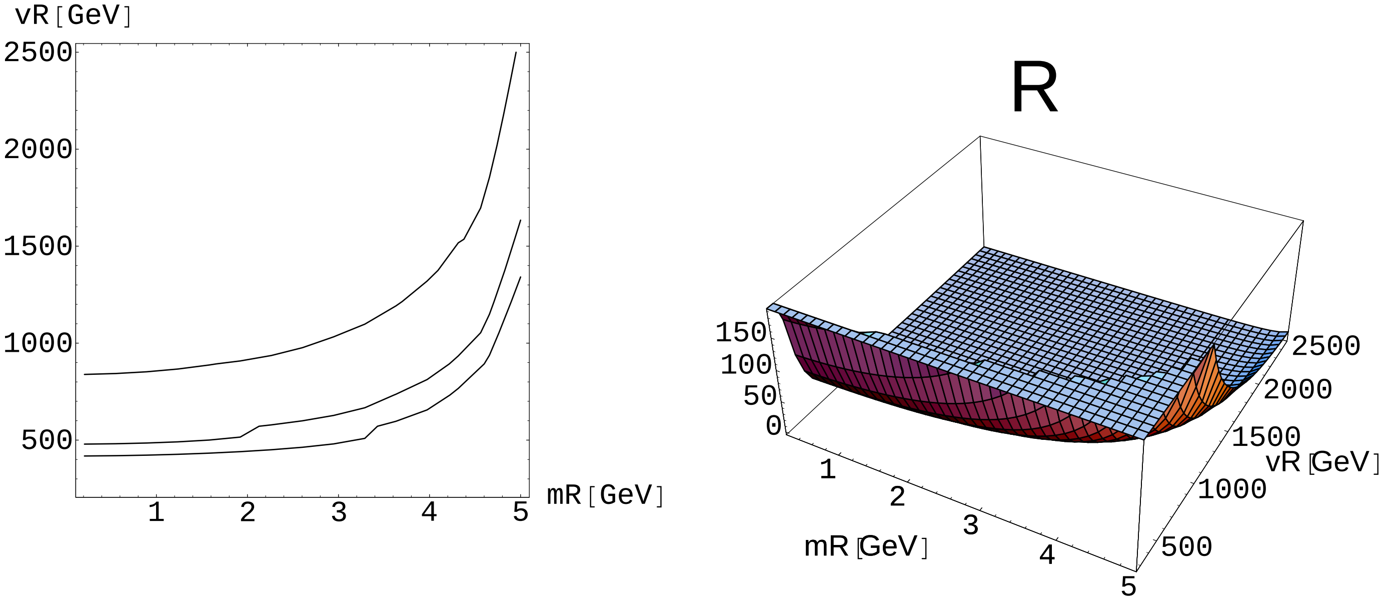

(a) (b)

Figure 4(a,b). *Figure 4a corresponds to the contour plots in the* $mR(m_\phi)$ *-*$vR(\langle\phi\rangle)$ *plane. Here* mR *and* vR *are in GeV unit. The contour line starting from the top to bottom corresponds to* $R = 10,\ 50$ *and* 100*, respectively. In Figure 4b, we have shown the variation of* R *with* mR *and* vR*.*

- For a given R curve, we see that the lower bound on $\langle\phi\rangle$ increases with m_ϕ. For example, consider the $R = 10$ curve of Figure 4a. As m_ϕ varies from 0.21 GeV to 5 GeV, $\langle\phi\rangle$ (the lower bound) changes from 844 GeV to 2620 GeV. Similarly for the $R = 100$ curve and for the above m_ϕ range, the lower bound on $\langle\phi\rangle$ varies from 421 GeV to 1342 GeV.

- In Figure 5 we have plotted $BR(\overline{B}_s \to \mu^+\mu^-)$ as a function of $\langle\phi\rangle$ for $m_\phi = 1$ GeV (lower curve) and 4 GeV (upper curve), respectively. The horizontal line, the present experimental upper bound($= 1.0 \times 10^{-7}$), suggest that the region allowed for $\langle\phi\rangle$ lies below the horizontal curve. This immediately allows one to obtain lower bound on $\langle\phi\rangle$ and we find for $m_\phi = 1(4)$ GeV, the lower bound is about 605(945) GeV.

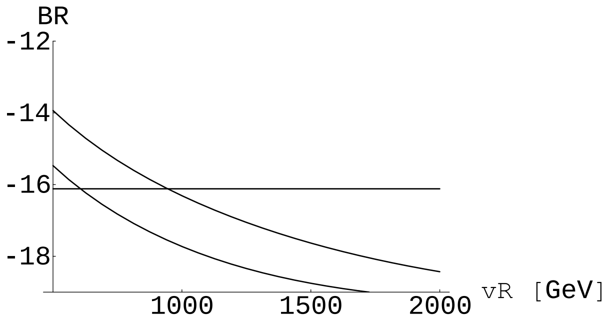

Figure 5. *In Figure 5, the* $BR(\overline{B}_s \to \mu^+\mu^-)$ *as a function of* $vR(\langle\phi\rangle)$ *(GeV) is shown. In y-axis we have actually plotted* $Log[BR(\overline{B}_s \to \mu^+\mu^-)]$. *For example,* $BR = -18(-14)$ *corresponds to* $1.523 \times 10^{-8}(8.315 \times 10^{-7})$. *The lower(upper) curve corresponds to* $m_\phi = 1(4)$ *GeV, respectively. The horizontal curve (corresponding to* $BR(\overline{B}_s \to \mu^+\mu^-) = 1.0 \times 10^{-7}$*) represents the present experimental upper bound. The region below the horizontal curve is allowed for* $vR(\langle\phi\rangle)$*.*

Invariant mass distribution

The invariant mass distribution is an useful probe to see the NP signal and we now obtain such a distribution to see the radion signal. In Figure 6, we have plotted $d\Gamma/dM_{\mu\mu}$ as a function of the $M_{\mu\mu}$ (the di-muon invariant mass), respectively for $\langle\phi\rangle = 247,\ 500$ GeV and 1 TeV (from top to bottom). The lowermost line corresponds to the SM background. Clearly for all $\langle\phi\rangle$ ranging from 247 GeV to 1 TeV, the signal is way above the SM background and the height of the resonance peak increases. To see these consider the curves corresponding to $m_\phi = 1$ GeV and $\langle\phi\rangle = 247, 500$ and 1000 GeV. One finds $d\Gamma/dM_{\mu\mu}$ as $\sim 5.5 \times 10^{-13}$, 8.55×10^{-13} and 1.03×10^{-12}, while for the SM one finds $d\Gamma/dM_{\mu\mu} = 4.62 \times 10^{-23}$. The detectibility ofcourse depends on the clarity of the peak structure. Since the decay width goes as $1/\langle\phi\rangle^2$, with the increase of $\langle\phi\rangle$, the resonance width decreases, one can have the better chance to see the resonance due to radion. We also see that with the increase of $\langle\phi\rangle$, resonance of higher radion mass gets lost and at $\langle\phi\rangle = 1$ TeV, resonance corresponding to $m_\phi = 1,\ 2$ GeV persists. We note that for $\langle\phi\rangle = 2$ TeV, the resonance corresponding to $m_\phi = 1$ GeV only survives (which is not shown in the figure).

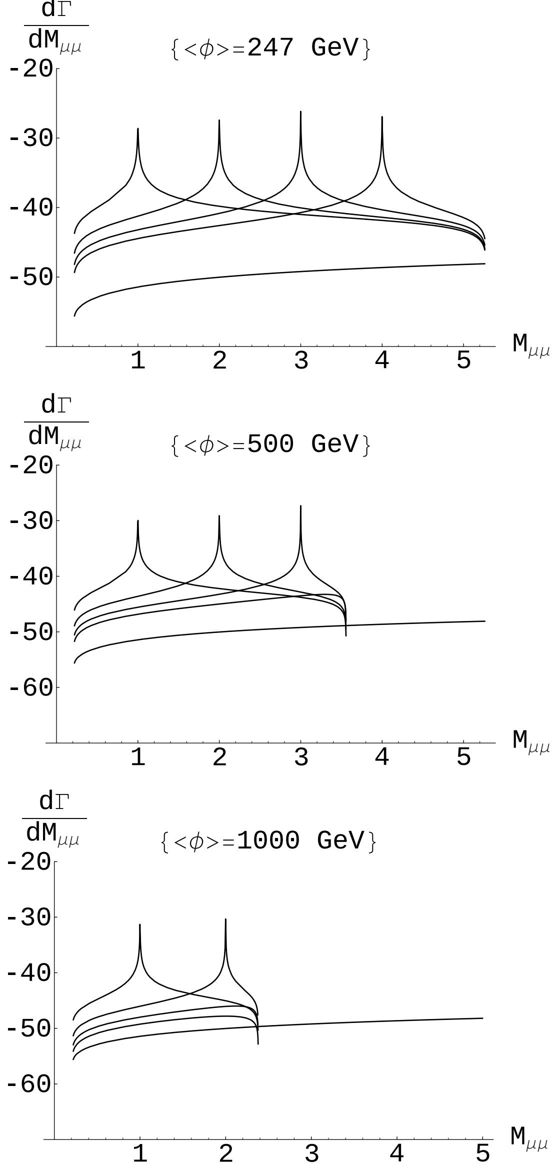

Figure 6. *Invariant mass distribution* $d\Gamma/dM_{\mu\mu}$ *for the ultra-light radion signal with* $m_\phi = 1, 2, 3$ *and* 4 *GeV (from left to right for a given curve), where the lowermost curve corresponds to the SM background. In y-axis we have actually plotted* $Log[d\Gamma(\overline{B}_s \to \mu^+\mu^-)/dM_{\mu\mu}]$. *The topmost,middle and lowermost curves corresponds to* $\langle\phi\rangle = 247,\ 500$ *GeV and* 1 *TeV, respectively.*

Comparison with other studies

We next compare our bound on $\langle\phi\rangle$ with that obtained from the muon anomaly data. The present BNL muon anomaly data tells $a_\mu^{(expt)} - a_\mu^{(SM)} = (28 \pm 10.5) \times 10^{-10}$. Fitting it with δa_μ^ϕ (radion contribution to muon anomaly) the author in [15] found the following bound for a relatively light radion: for $m_\phi = 2$ GeV, the lower bound on $\langle\phi\rangle$ is ~ 500 GeV corresponding to $\delta a_\mu^\phi = 3.85 \times 10^{-9}$ and ~ 760 GeV for $\delta a_\mu^\phi = 1.75 \times 10^{-9}$. The upper bound on $BR(\overline{B}_s \to \mu^+\mu^-)$ suggests a lower bound about 918 GeV (corresponding to $R = 10$) ~ 459 GeV (corresponding to $R = 100$) for $m_\phi = 2$ GeV and is in agreement with that obtained from the muon anomaly data as mentioned above.

5 Summary and Conclusion

We analyse the $\overline{B}_s \to \mu^+\mu^-$ decay in the Randall-Sundrum model in the presence of an ultra-light stabilized radion. Using the present experimental bound of the branching ratio $BR(\overline{B}_s \to \mu^+\mu^-)$ (two order larger than the standard model result), we obtain contour plots in the $m_\phi - \langle\phi\rangle$ plane. For $BR(\overline{B}_s \to \mu^+\mu^-) = 1.0 \times 10^{-7}$ and radion mass $m_\phi = 0.21(5)$ GeV, we obtain the lower bound on $\langle\phi\rangle$ about 844(2620) GeV corresponding to $R = 10$ and about 421(1342) GeV corresponding to $R = 100$. We have shown the invariant mass ($M_{\mu\mu}$) distribution plot which clearly shows the existence of the radion signal. The SM background on which the radion signal lies is highly suppressed. Finally, we compare our result with the bound obtained from the BNL muon anomaly data and found some agreement between the two.

6 Acknowledgments

We would like to thank Prof.R. Sinha of IMSc, Chennai for correcting our mistakes and his several useful comments related to this work. P.K.D would like to thank Prof.Uma Mahanta(late) who first introduced the author to the beauty of the Brane World Physics.

A SM amplitude of the process $\overline{B}_s \to \mu^+\mu^-$

In this appendix, we calculate the square of the SM amplitude of $\overline{B}_s \to \mu^+\mu^-$ (at the quark level it yields $b\overline{s} \to \mu^+\mu^-$ process) of Eq.(9). We define p_b, p_s, p_1 and p_2 to be the momenta of the b-quark, s-quark, μ^+ and μ^-, respectively and m_μ, the muon mass and $q = p_b + p_s = p_1 + p_2$. The individual amplitude-square elements are listed below:

$$\begin{aligned}\overline{|\mathcal{M}_{10}|^2} \;=\;& C'|C_{10}|^2[4{m_\mu}^2{m_b}^2 - 4(p_1.p_2){m_b}^2 + 4{m_\mu}^2{m_s}^2 - 4(p_1.p_2){m_s}^2 \\ &+8(p_1.p_b)(p_2.p_b) + 8(p_1.p_s)(p_2.p_b) + 8(p_1.p_b)(p_2.p_s) + 8(p_1.p_s)(p_2.p_s) \\ &+8{m_\mu}^2(p_b.p_s) - 8(p_1.p_2)(p_b.p_s)]. \qquad (21)\end{aligned}$$

where the prefactor C' is defined as follows

$$C' = (\frac{\alpha G_F f_{\overline{B}_s}}{2\pi\sqrt{2}})^2|V_{tb}|^2|V_{ts}|^2. \qquad (22)$$

B NP contribution

B.1 Interaction vertex of Radion and SM particle

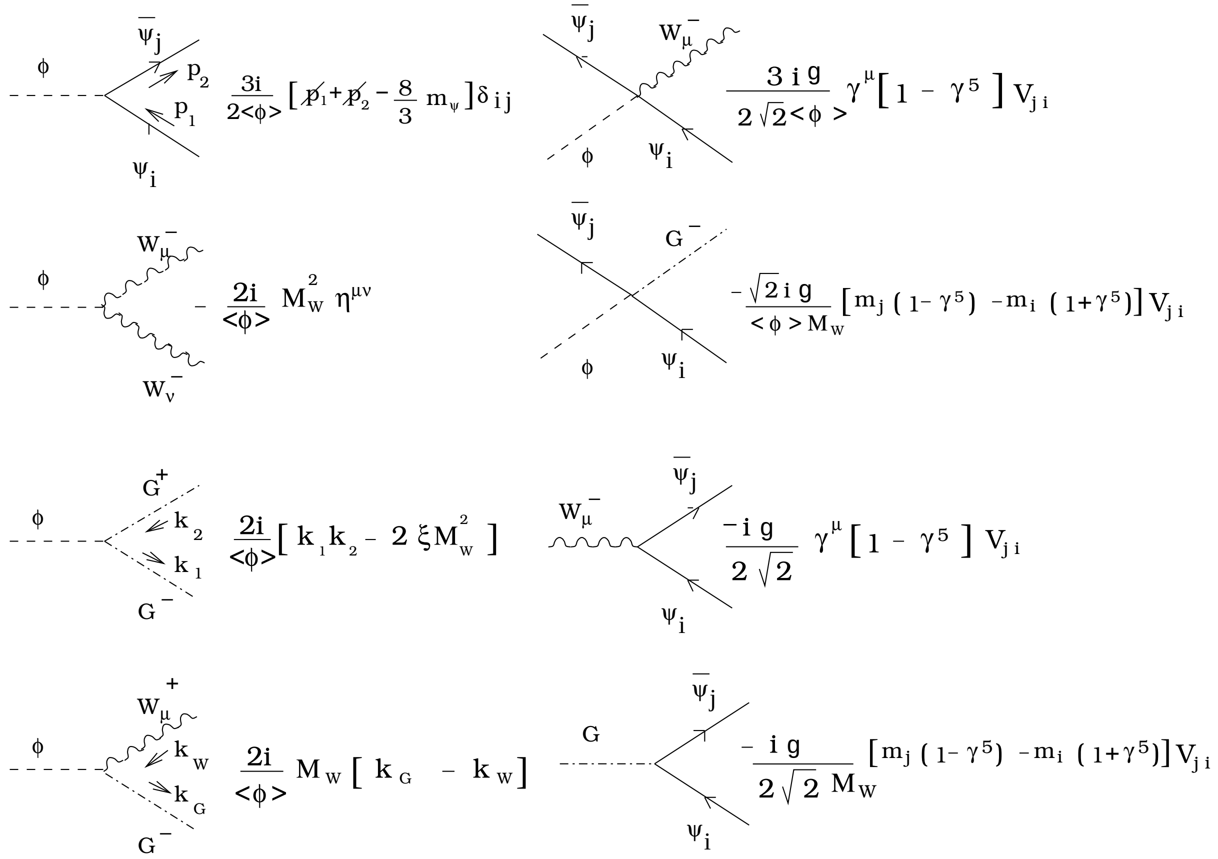
ϕ
$\bar{\psi}_j$
p_2
p_1
ψ_i
$\frac{3i}{2<\phi>}[\not{p}_1+\not{p}_2-\frac{8}{3}m_\psi]\delta_{ij}$
$\bar{\psi}_j$
W_μ^-
ϕ
ψ_i
$\frac{3ig}{2\sqrt{2}<\phi>}\gamma^\mu[1-\gamma^5]V_{ji}$
W_μ^-
ϕ
W_ν^-
$-\frac{2i}{<\phi>}M_W^2\eta^{\mu\nu}$
$\bar{\psi}_j$
G^-
ϕ
ψ_i
$-\frac{\sqrt{2}ig}{<\phi>M_W}[m_j(1-\gamma^5)-m_i(1+\gamma^5)]V_{ji}$
G^+
ϕ
k_2
k_1
G^-
$\frac{2i}{<\phi>}[k_1k_2-2\xi M_W^2]$
W_μ^-
$\bar{\psi}_j$
ψ_i
$\frac{-ig}{2\sqrt{2}}\gamma^\mu[1-\gamma^5]V_{ji}$
W_μ^+
ϕ
k_W
k_G
G^-
$\frac{2i}{<\phi>}M_W[k_G-k_W]$
G
$\bar{\psi}_j$
ψ_i
$-\frac{ig}{2\sqrt{2}M_W}[m_j(1-\gamma^5)-m_i(1+\gamma^5)]V_{ji}$

Figure 1: The relevant diagrams of the interaction vertex of Radion and SM particles in the R_ξ gauge.

B.2 Feynman diagrams of the Radion penguin with SM particles.

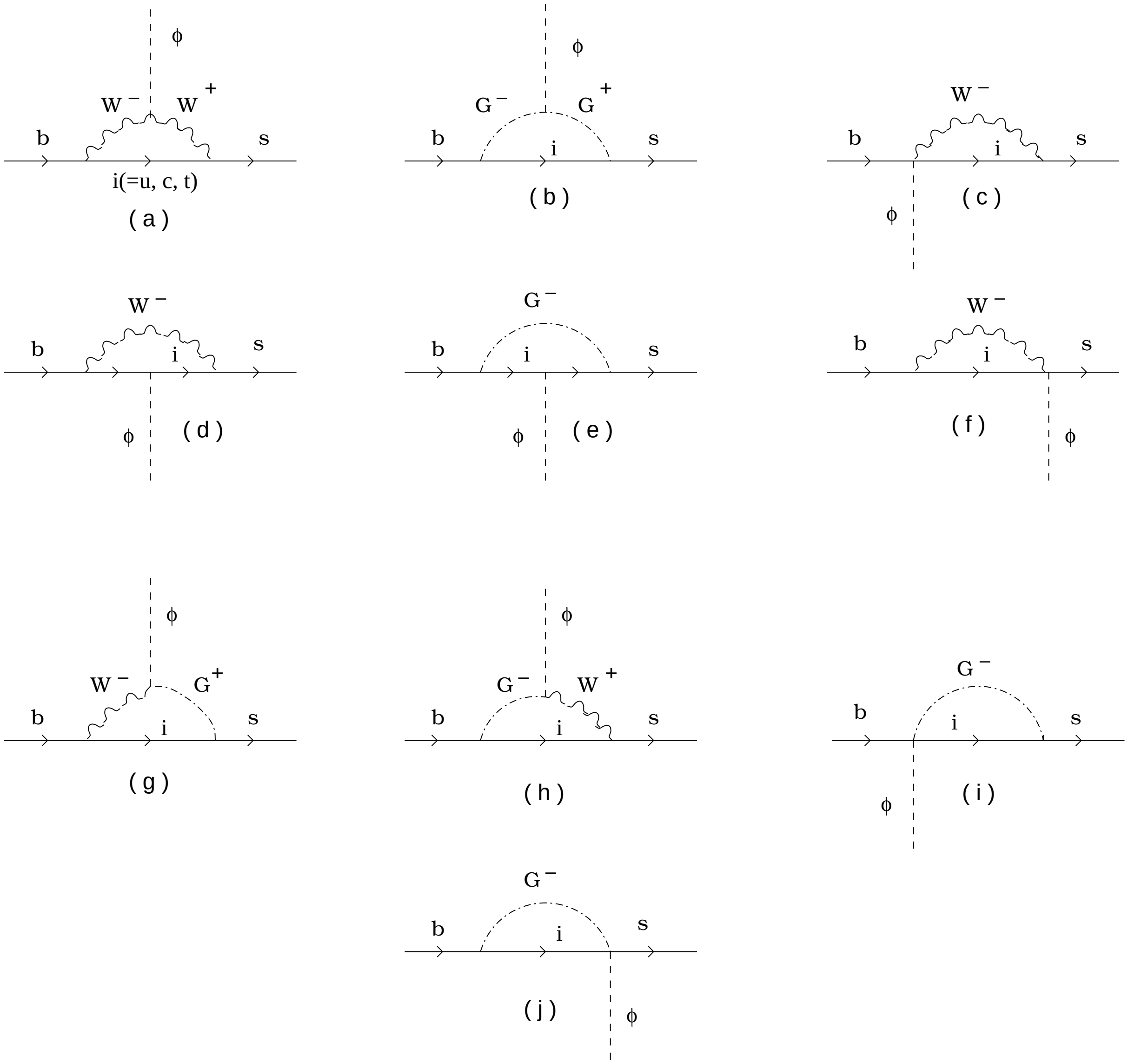

Figure 2: The Feynman diagrams of the Radion penguin with SM particles in the general R_ξ gauge .

B.3 NP amplitude of the process $\overline{B}_s \to \mu^+\mu^-$

In this appendix, we calculate the square of the NP amplitude of $\overline{B}_s \to \mu^+\mu^-$ of Eq.(14). The individual amplitude-squared elements are given by

$$\begin{aligned} \overline{|\mathcal{M}_{NP}|^2} &= C_L(p_1.p_2 - {m_\mu}^2), && (23) \\ \overline{2Re(\mathcal{M}_{10}^\dagger \mathcal{M}_{NP})} &= 0, && (24) \end{aligned}$$

where

$$\begin{aligned} C_L &= |V_{tb}|^2 |V_{ts}|^2 \left(\frac{G_F m_b m_\mu \mathcal{L}_\phi}{\sqrt{2}\langle\phi\rangle} \right)^2 \left(\frac{f_{\overline{B}_s} {m_{\overline{B}_s}}^2}{m_b + m_s} \right)^2 \times \frac{1}{(q^2 - m_\phi^2)^2 + \Gamma_\phi^2 m_\phi^2}, \\ \mathcal{L}_\phi &= \frac{{m_t}^2}{2\pi^2\langle\phi\rangle} \int_0^1 F(x) dx. \end{aligned}$$

In above

$$\begin{aligned} F(x) &= 4(Log(\Lambda^2/A^2) - 1) + \frac{x{m_t}^2}{A^2} + \frac{(1-x){M_W}^2}{A^2}, \\ \Lambda &= 4\pi\langle\phi\rangle, \quad A^2 = x{m_t}^2 + (1-x){M_W}^2. \end{aligned}$$

We worked in the ‘t-Hooft Feynman gauge ($\xi = 1$).

References

[1] N. Arkani-Hamed, S. Dimopoulos and G. Dvali, *Phys. Lett.* **B 429** , 263 (1998); I. Antoniadis, N. Arkani-Hamed and G. Dvali, *Phys. Lett.* **B 463**, 257 (1998).

[2] L. Randall and R. Sundrum, *Phys. Rev. Lett.* **83**, 3370 (1999), *Phys. Rev. Lett.* **83**, 4690 (1999).

[3] W. D. Goldberger and M. B.Wise, *Phys. Rev. Lett.* **83** , 4922 (1999); W. D. Goldberger and M. B.Wise, *Phys. Rev.* **D 60** , 107505 (1999); G. F. Giudice, R. Rattazzi and J. D. Wells, *Nucl. Phys.* **B 595**, 250 (2001); W. D. Goldberger and M. B.Wise, *Phys. Lett.* **B 475**, 275-279 (2000); W. D. Goldberger and I. Z. Rothstein, *Phys. Lett.* **B 491**, 339 (2000).

[4] M. L. Graesser, hep-ph/9902310; U. Mahanta and S. Rakshit, *Phys. Lett.* **B 480**, 176 (2000); S. C. Park and H. S. Song, *Phys. Lett.* **B 506**, 99 (2001); C. S. Kim, J. D. Kim and J. Song, *Phys. Lett.* **B 511**, 251 (2001); C. Csaki, M. Graesser, L. Randall and J. Terning, *Phys. Rev.* **D 62**, 045015 (2000); U. Mahanta and A. Datta, *Phys. Lett.* **B 483**, 196 (2000); S. Bae, P. Ko, H. Lee and J. Lee, *Phys. Lett.* **B 487**, 299 (2000); K. Cheung, *Phys. Rev.* **D 63**, 056007 (2001); P. K. Das and U. Mahanta, *Phys. Lett.* **528**, 253 (2002), *Mod. Phys. Lett.* **A**, 127 (2004), hep-ph/0201260, hep-ph/0202193; M. Chaichian, A. Datta, K.Huitu and Z. Yu, *Phys. Lett.* **B 524**, 161 (2002); S. V. Demidov and D. S. Gorbunov, *Phys. Atom. Nucl* **69**, 712 (2006); S. M. Letti, *Phys. Lett.* **B 540**, 252 (2002); M Battaglia *et al*, *Phys. Lett.* **B 568**, 92 (2003); P. K. Das and B. Mukhopadhyaya, hep-ph/0303135; P. K. Das,*Phys. Rev.* **D 72**, 055009 (2005).

[5] See the website http://www.slac.stanford.edu/xorg/hfag/rare/winter06/bs/index.html, for the recent information on B_s meson decay and the eprint hep-ex/0603003 by the Heavy Flavor Averaging Group.

[6] A. J. Buras, *Phys. Lett.* **B 566**, 115 (2003); G. Buchalla, A. J. Buras and M. E. Lautenbacher *Rev. Mod. Phys.* **68**, 1125 (1996).

[7] A. Ali *et al* *Phys. Rev.* **D 55**, 4105 (1997); A. J. Buras and M. Munz, *Phys. Rev.* **D 52**, 186 (1995); M. Misiak, *Nucl. Phys.* **B 393**, 23 (1993); *Nucl. Phys.* **B 439**, 461 (1995), S. R. Choudhury and N. Gaur, *Phys. Lett.* **B 451**, 86 (1999).

[8] T P. Cheng and L. F. Li, Gauge theoy of elementary particle physics, Clarendon Press, Oxford, 1984 (see it's appendix).

[9] U. Mahanta and S. Mohanty *Phys. Rev.* **D 62**, 083003 (2000).

[10] G. Giudice *et al* *Nucl. Phys.* **B 595**, 250 (2001).

[11] S. K. Rai, P. K. Das and S. Rauchaudhuri, *Phys. Lett.* **B 618**, 221 (2005); P. K. Das, *Phys. Rev.* **D 72**, 055009 (2005).

[12] Particle Data Group *Phys. Lett.* **B 592**, 1 (2004).

[13] CKMfitter Group (J.Charles *et al*) *Eur. Phys.* **J C41**, 1 (2005), updated in http://ckmfitter.in2p3.fr.

[14] H. Y. Cheng and K.C. Yang, *Phys. Lett.* **B 511**, 40 (2001)

[15] P. K. Das,hep-ph/0407041, P. K. Das and U. Mahanta, *Nucl. Phys.* **B 644**, 395 (2002).